Interference Effects in Three-Terminal Hybrid Systems with Quantum Dots

G. Michałek and B.R. Bułka

Institute of Molecular Physics, Polish Academy of Sciences, M. Smoluchowskiego 17, 60-179 Poznań, Poland

Conductance in a three-terminal hybrid system with two quantum dots is analyzed. Our attention is focused on an influence of decoherence on interference effects in the Andreev transport. In particular, we have found that a change of coupling to the third electrode can strongly modify a shape of the Fano-type resonances. This effect is due to activation of nonlocal Andreev reflection (CAR) processes.

1. Introduction

In recent years a lot of attention is devoted to hybrid nanodevices with a quantum dot (QD) [2] coupled to a normal-metal (N) and a superconducting (S) electrode. These structures show competition between various processes like conventional electron and the Cooper pair tunnelling or the Andreev reflection [1, 2], as well as interference effects in double quantum dot [3, 4]. Very promising are three terminal devices, where a side terminal gives a possibility to control, manipulate or detect currents between remaining terminals [5, 6]. It was demonstrated by Hofstetter et al. [7] that the double quantum dot connected to two normal-metal contacts and a central superconducting finger acts as tunable Cooper pair splitter.

In the paper we focus on a quantum interference and an influence of decoherence in a three-terminal system. In particular, we identify processes, which are responsible for the Fano-type resonances and changes of the shape of the conductance characteristics. Moreover, we show that the side electrode can completely destroy the quantum interference and proximity effects.

2. Description of the three-terminal hybrid system

We consider a device, which is composed of two quantum dots (QDs) coupled with normal-metal left (L) and right (R) electrodes. Furthermore one of the QD is connected with S lead, see inset in Fig. 1a. In order to get a clear picture of the physics we neglect the Coulomb interaction on QDs. Moreover, we assume that an applied bias voltage V_L is small, so only one single degenerate energy level ϵ_1 (ϵ_2) of the first (the second) QD lies in the transport window. The bias voltage V_L is applied to the left electrode, while the right and superconducting electrodes are grounded. The S electrode is built from the BCS-type superconductor with an energy gap Δ. The normal-metal electrodes are treated in the wide-band approximation. Electron and hole transfer between the QDs and the adjacent leads is described by a set of tunnelling rates Γ_i ($i = \{L, R, S\}$), whereas the inter-dot coupling is governed by the hopping integral t_{12}.

Currents flowing into the QD1 from the L electrode can be calculated from the evolution of the total number operator using the equation of motion technique (EOM) for the non-equilibrium Green function [8, 9]. In calculations one can separate currents originating from various types of tunnelling processes. For voltages $|eV| < \Delta$ only two components survive

$$I_L^{ET} = \frac{2e}{\hbar} \int \frac{dE}{2\pi} \Gamma_L \Gamma_R |G_{11}^r|^2 (f_L - f_R),$$

$$I_L^{AR} = \frac{2e}{\hbar} \int \frac{dE}{2\pi} \Gamma_L |G_{12}^r|^2$$
$$\times \left[\Gamma_L \left(f_L - \tilde{f}_L \right) + \Gamma_R \left(f_L - \tilde{f}_R \right) \right], \tag{1}$$

where I_L^{ET} denotes the current due to the normal electron transfer processes, while I_L^{AR} is the Andreev current caused by the Andreev reflection. f ($\tilde{f}$) denotes the Fermi energy for an electron (hole). The Green functions G_{11}^r and G_{12}^r can be written in the form

$$G_{11}^r = \frac{1}{E - \epsilon_1 - \Sigma_{11}^r - \frac{|\Sigma_{12}^r|^2}{E + \epsilon_1 - \Sigma_{22}^r}},$$

$$G_{12}^r = -\frac{\Sigma_{12}^r}{E + \epsilon_1 - \Sigma_{22}^r} G_{11}^r, \tag{2}$$

where the self energies Σ_{ij}^r ($i, j = \{1, 2\}$):

$$\Sigma^r = \begin{pmatrix} -\frac{i}{2}\beta\Gamma_S - \frac{i}{2}\Gamma_L + \frac{t_{12}^2}{E - \epsilon_2 + i\Gamma_R/2} & \frac{i}{2}\frac{\Delta}{E}\beta\Gamma_S \\ \frac{i}{2}\frac{\Delta}{E}\beta\Gamma_S & -\frac{i}{2}\beta\Gamma_S - \frac{i}{2}\Gamma_L + \frac{t_{12}^2}{E + \epsilon_2 + i\Gamma_R/2} \end{pmatrix} \tag{3}$$
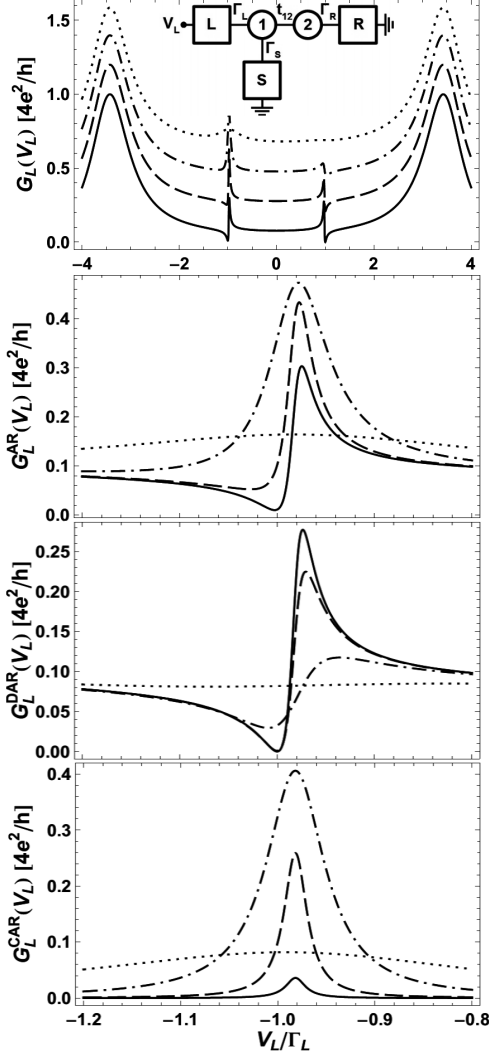
Fig. 1. (a) $\mathcal{G}_L$ (curves are shifted in vertical for clarity), (b) $\mathcal{G}_L^{AR}$, (c) $\mathcal{G}_L^{DAR}$ and (d) $\mathcal{G}_L^{CAR}$ as a function of the bias voltage V_L for different couplings to the right lead: $\Gamma_R = 0.0005\Gamma_L$ (solid), $\Gamma_R = 0.005\Gamma_L$ (dash), $\Gamma_R = 0.05\Gamma_L$ (dash-dot), $\Gamma_R = 0.5\Gamma_L$ (dot). The other parameters are $\Gamma_S = 7\Gamma_L$, $t_{12} = 0.5\Gamma_L$, $\epsilon_1 = 0$, $\epsilon_2 = \Gamma_L$, $\Delta \gg \Gamma_S$, $T = 0$. Γ_L is taken as unity in our calculations.

and $\beta = \frac{E}{i\sqrt{\Delta^2 - E^2}}$ inside the superconducting energy gap Δ.

From the currents (1) one can find differential conductances $\mathcal{G}_L^{ET/AR} \equiv dI_L^{ET/AR}/dV_L$.

3. Results and conclusions

We calculated the conductance $\mathcal{G}_L = \mathcal{G}_L^{ET} + \mathcal{G}_L^{AR}$ as a function of the bias voltage V_L at the temperature of $T = 0$. The studies focused on the devices with large tunnel coupling asymmetry $\Gamma_S > \Gamma_L$. The results are presented in Fig. 1a for several couplings to the right electrode. In this case one can see two wide, well separated peaks near quasiparticle energies $\pm\sqrt{\epsilon_1^2 + \Gamma_S^2/4}/\Gamma_L \approx \pm 3.5$. These

peaks are signatures of the particle–hole splitting of the quasiparticle level ϵ_1 due to the proximity effect on QD1. Between large peaks one can see additional features at $eV_L = \pm\epsilon_2$, which appear due to quantum interference, Fig. 1a. For the small $t_{12} < \Gamma_L$ interference is manifested in $\mathcal{G}_L$ as the narrow resonances with characteristic Fano-type line shape [3]. For the larger $t_{12} > \Gamma_L$ the proximity effect is clearly visible in $\mathcal{G}_L$ as two additional peaks with destructive interference lowering conductance between them (not shown).

Let us analyze now resonance at $-\epsilon_2$. For small coupling t_{12} the contribution from the ET processes is at least two orders of magnitude smaller than the contribution from the AR processes and can be neglected. Therefore in Fig. 1b we have plotted only the Andreev conductance $\mathcal{G}_L^{AR}$. For the small Γ_R the resonance has a Fano-type line shape, Fig. 1b. For the larger Γ_R one can observe transformation to a single broad peak, Fig. 1b. For a very large Γ_R the peak is smeared out. This is an effect of competition between different Andreev reflection processes.

It is well known that in three terminal hybrid systems one can observe two types of the Andreev scattering. In the direct Andreev reflection (DAR) processes an electron from the left electrode is converted into a Cooper pair in the superconductor while at the same time a hole is reflected back to the left electrode. In the crossed Andreev reflection (CAR) the hole is transferred to the right electrode. The total Andreev conductance can be written as $\mathcal{G}_L^{AR} = \mathcal{G}_L^{DAR} + \mathcal{G}_L^{CAR}$. It is worth to notice that CAR processes are activated only near $-\epsilon_2$ while DAR processes contribute to conductance in whole voltage range. The results for $\mathcal{G}_L^{DAR}$ and $\mathcal{G}_L^{CAR}$ near $-\epsilon_2$ are plotted in Fig. 1c and d, respectively. The amplitude of $\mathcal{G}_L^{DAR}$ decreases with an increase of Γ_R and its line shape is the Fano-type in the wide range of parameter Γ_R, Fig. 1c. On the other side, the contribution from the CAR processes increases with an increase of Γ_R while $\mathcal{G}_L^{CAR}$ has always the line shape of the peak, Fig. 1d. For a small Γ_R the amplitude of $\mathcal{G}_L^{DAR}$ is larger than the amplitude of $\mathcal{G}_L^{CAR}$, therefore the Fano line shape of $\mathcal{G}_L^{AR}$ is determined by $\mathcal{G}_L^{DAR}$. For larger Γ_R the peak in $\mathcal{G}_L^{AR}$ is due to activation of the CAR processes. CAR competes with interference processes caused by hopping between QDs. Decoherence introduced through the right lead destroys Fano-type resonances in $\mathcal{G}_L^{DAR}$, Fig. 1c. When $\Gamma_R \gg t_{12}$ also the peaks in the $\mathcal{G}_L^{CAR}$ are washed out, Figs. 1d.

Summarizing, in the paper we analyzed the influence of CAR processes on the interference in three-terminal hybrid devices with coupled QDs and on the shape of current–voltage characteristics.

References

[1] S. De Franceschi, L. Kouwenhoven, Ch. Schönen-berger, W. Wernsdorfer, *Nat. Nanotechnol.* **5**, 703 (2010).

[2] A. Martín-Rodero, A.L. Yeyati, *Adv. Phys.* **60**, 899 (2011).

[3] J. Barański, T. Domański, *Phys. Rev. B* **84**, 195424 (2011).

[4] J. Barański, T. Domański, *Phys. Rev. B* **85**, 205451 (2012).

[5] B. Sothmann, D. Futterer, M. Governale, J. König, *Phys. Rev. B* **82**, 094514 (2010).

[6] R. Lü, H.-Z. Lu, X. Dai, J. Hu, *J. Phys., Condens. Matter* **21**, 495304 (2009).

[7] L. Hofstetter, S. Csonka, J. Nygård, C. Schoönen-berger, *Nature* **461**, 960 (2009).

[8] H.J.W. Haug, A.-P. Jauho, *Quantum Kinetics in Transport and Optics of Semiconductors*, Springer, Berlin 2008.

[9] C. Niu, D.L. Lin, T.-H. Lin, *J. Phys., Condens. Matter* **11**, 1511 (1999).